The CMS PbWO_4 electromagnetic calorimeter

M. Lethuillier

Available on CMS information server **CMS CR 2003/0042**

CMS Conference Report

24 September 2003

The CMS $PbWO_4$ Electromagnetic Calorimeter

M. Lethuillier

Institut de Physique Nucléaire, Lyon

Abstract

The electromagnetic calorimeter under construction for the CMS experiment at LHC will be the largest crystal calorimeter ever built. The very fast and precise energy measurement of electrons and photons is based upon 76000 lead tungstate crystals read by avalanche photodiodes (APD) in the central barrel region and vacuum phototriodes (VPT) in the endcap regions. The major challenges to be faced are the ability to operate in a strong magnetic field of 4T and under unprecedented radiation levels, the LHC bunch crossing time of 25 ns, the need for a precise energy measurement over a very large dynamic range, from approximately 50 MeV to more than 1 TeV, and the high reliability required of the full on-board readout chain which will be inaccessible after the start of LHC in 2007. A review of the calorimeter design is given and the current status of the construction is reported. Highlights of results obtained during beam tests are also presented.

Presented at *ASI Praha - Physics at LHC*, Prague, July 6-12, 2003.

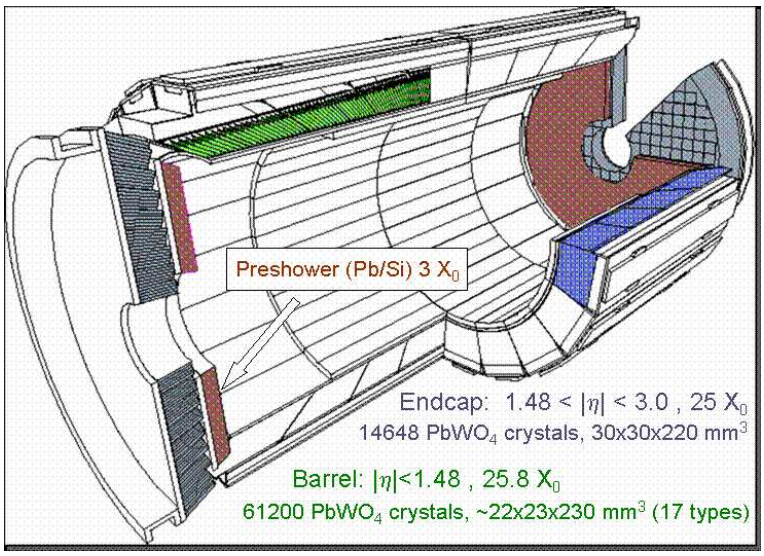

Figure 1: View of the CMS electromagnetic calorimeter

1 Introduction

Understanding electroweak symmetry-breaking is a key goal of the LHC. The Higgs boson will be searched in 14 TeV proton-proton collisions at a crossing rate of 40 MHz and a nominal luminosity of 10^{34} $\mathrm{cm}^{-2}\mathrm{s}^{-1}$. In the low-mass region ($\mathrm{m_H} \lesssim 140\mathrm{GeV/c^2}$) favoured by electroweak precision measurements [1], the dominant decay channel $\mathrm{H} \to \mathrm{b\bar{b}}$ suffers from a very large QCD background and from its reliance on jet energy resolution which is relatively poor ($\sim$ 15%). In this region, the natural Higgs width is very small, and its mass resolution is dominated by the detector resolution. An extremly precise angular and energy measurement of photons would permit a sufficiently high S/N ratio to compensate the low branching ratio of the "golden" discovery channel $\mathrm{H} \to \gamma\gamma$. The CMS collaboration has opted for a calorimeter [2] composed of 61200 $PbWO_4$ crystals off-pointing by 3° in both η and ϕ in the barrel region and 14648 $PbWO_4$ crystals in the endcaps, as shown in figure 1. A fine-grained preshower detector is placed in front of the endcap crystals to improve the π^0/γ discrimination and help the vertex reconstruction. It consists of two layers of lead absorber (3 X_0) and two orthogonal planes of silicon strip detectors with 1.9 mm pitch [3].

2 Crystals

The choice of lead tungstate crystals was driven by their short radiation length (0.89 cm) and their small Molière radius (2.19 cm). This allows the calorimeter to be sufficiently compact to be inserted within the magnet coil (avoiding degradation of the resolution) and sufficiently fine-grained for π^0 separation. Its fast scintillation time (light decay time of $\sim$ 10 ns, 80% of the light collected in 25 ns) is fully compatible with the high LHC event rate (around 20 pile-up events per 25 ns bunch crossing). The peak scintillation emission at 420 nm is compatible with photodetection. The drawback is a low light yield (three orders of magnitude less than of NaI) strongly dependent on temperature (-2%/degree at $+18°$), thus requiring photodetectors with intrinsic amplification and an operating temperature stable to $\pm 0.1°$. The hostile radiation environment (0.15-0.3 Gy/hour in the barrel and 0.3-15 Gy/hour in the endcap) sets drastic constraints on radiation hardness of the $PbWO_4$ crystals. Intensive R&D has been conducted to study radiation damage. Neither the scintillation mechanism nor the emission spectrum are affected by the radiation. Only a loss of transparency is observed, due to the formation of color centers [4]. Stochiometric fine tuning, Y/Nb doping and optimized growth conditions have improved the radiation hardness and the light transmission. The R&D has also succeeded in increasing the light yield well above the specification limit of 8 photoelectrons/MeV and in reducing its non-uniformity (by depolishing and shading) under the limit of 3.5%/X_0, equivalent to a contribution of 0.3% to the constant term of the resolution. Figure 2 illustrates the performance of production crystals. The crystals are being supplied by the Bogoroditsk Techno-Chemical Plant (BTCP). The growth of large ingots (85 mm diameter) is now well mastered, and the ovens have been upgraded to this capability. Important progress has also been achieved in the cutting technique. Square endcuts and longitudinal precuts on 1/3 of diameter before annealing and a final cut after annealing should permit the production of 4 barrel crystals or 2 endcap crystals per 85 mm ingot. So far 16000 barrel crystals have been delivered.

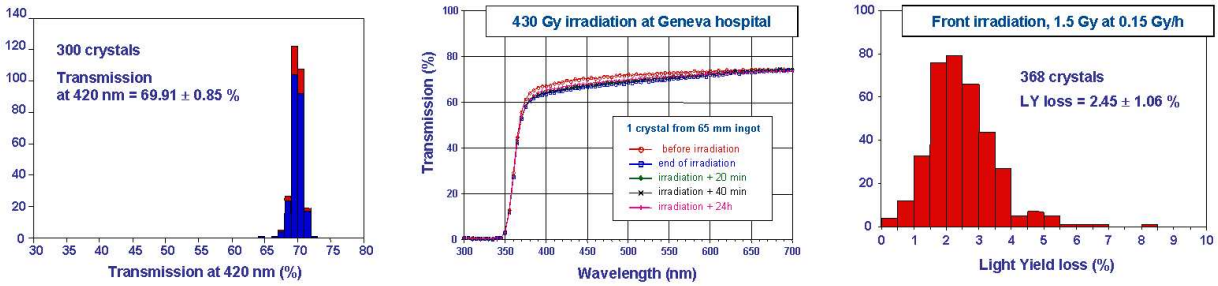

Figure 2: Left: Distribution of the longitudinal transmission at peak scintillation emission for 300 production crystals. The mean value of 70% is well above the minimum acceptable of 55%. Center: Tansmission curve after and before a 430 Gy irradiation of one crystal. Right: Distribution of the light yield loss after a 1.5 Gy irradiation for 368 crystals.

3 Photodetectors

The relatively low light yield of $PbWO_4$ requires the use of photodetectors with internal gain. In the central barrel region, the strong magnetic field normal to the crystal axis forbids the use of photomultiplier tubes or phototriodes. A 10-year R&D effort in collaboration with Hamamatsu Photonics resulted in the conception of the CMS avalanche photodiode (APD). The principle of operation is shown in figure 3. Two APDs connected in parallel are mounted on the rear face of the crystal providing a 50 mm^2 active area. With an effective silicon thickness of around 6 μm, the APDs are rather insensitive to rear shower leakage. The APDs are operated at a gain of 50 (gains in excess of 1000 are possible). The APD contributes to all three resolution terms. The active area, the quantum efficiency ($\sim$75% at the peak emission wavelength of $PbWO_4$) and the excess noise factor (F=2 at gain 50) contribute to the stochastic term, the APD capacitance ($\sim$80 pF) and dark current contribute to the noise term, and the stability of the gain (strongly dependent (3%/V) on the bias voltage and on temperature (-2.2%/degree)) contributes to the constant term through intercalibration effects. Once mounted inside the calorimeter, the APDs will be inaccessible for the 10-year life of the experiment, requiring a 99.9% reliability. Each APD is selected after a strict screening program [5] involving a 500 krad pre-irradiation with a Co^{60} source followed by annealing and accelerated ageing under bias. The APD production is well underway with more than 85 000 pieces delivered of a total of 130 000.
In the endcap, the radiation level, orders of magnitude higher than in the barrel, forbids the long-term use of APDs. The favourable orientation of the magnetic field ($8.5° < \theta < 25.5°$ between the field and the photodetector axis) leads to the choice of vacuum phototriodes (VPT) [6], single stage photomultiplier tubes with fine-mesh anodes (100 lines/mm) as represented in figure 4. Equipped with UV glass windows, they are far more radiation-hard than silicon diodes (the window transmission loss after 10 years of LHC running is less than 10%). They have an external radius of 26.5 mm, an effective photocathode area of 280 mm^2 and a quantum efficiency of around 20% at the peak emission wave length of lead tungstate. The gain provided is of order 8-10 in a magnetic field of 4T, the excess noise factor is around 3 and the response is uniform for the range of angles their axes make with

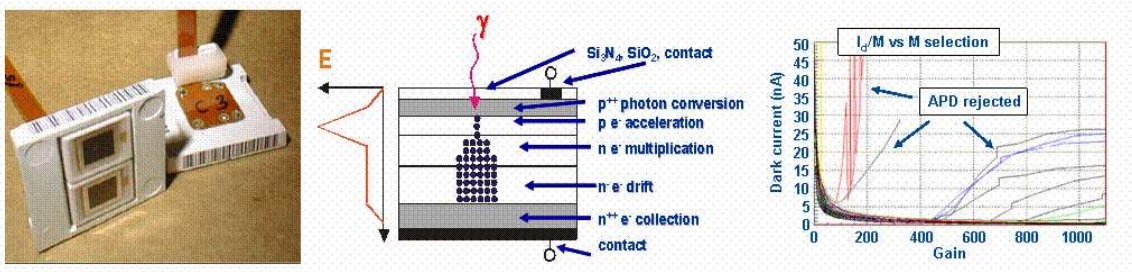

Figure 3: Left: Photo of the photodetection "capsule" which consists of two silicon avalanche photodiodes (APD) and, on one of every ten, a temperature sensor. Center: Principle of operation of an APD. Right: The dark current normalized to gain (M) vs. gain curve is one of the criteria for APD selection.

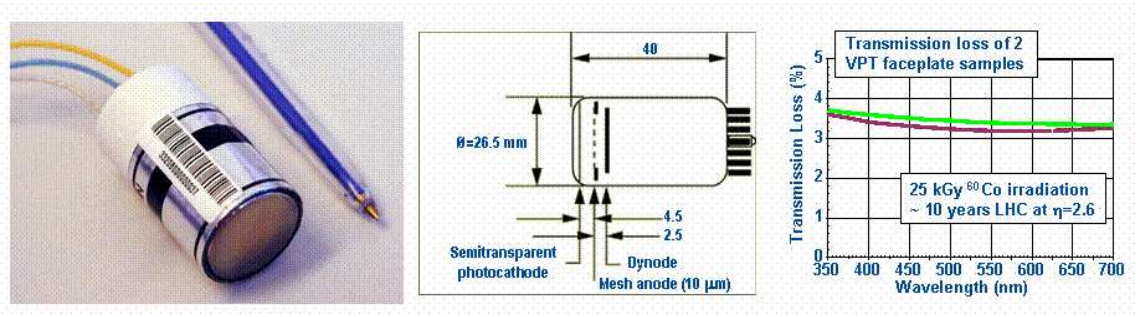

Figure 4: Left and center: Photo and schematic view of a VPT. Right: Transmission loss of two VPT faceplates vs. wavelength after a 25 kGy irradiation.

the magnetic field direction. On receipt, all VPTs are tested in a magnetic field of 1.8T at a number of angles in the range from 0 to 35° with respect to the field direction. A 10% subsample is also studied at 4T and 15°. Sample batches of faceplate glass are irradiated with gamma-rays to 20 kGy to confirm the radiation hardness. The production by the RIE corporation in St Petersburg is well advanced with 1/3 of the 15500 VPTs already delivered.

4 Electronic Readout System

The objectives for the front-end (FE) electronics are extremely challenging. The electronics must be extremely fast to match the 25 ns LHC crossing rate. Because of the low S/N-ratio signals (low light yield of the lead tungstate), it must provide a very precise energy measurement on a dynamic range as large as $\sim$ 95 dB. The noise has to be kept below $\sim$ 100 MeV per crystal in the central region. Placed on the detector, the FE electronics must be radiation-hard and reliable. These tight constraints have required the development of custom integrated circuits.

The years 2002-2003 saw two major changes in the electronic design. In the "old" design, each photodetector (APD or VPT) provides signals to a FPPA (Floating Point PreAmplifier) made in the complementary UHF1x bipolar technology from Intersil. The large dynamic range of $\sim$ 95 dB ($\sim$ 50 MeV (noise) - 1.5 TeV) needed to satisfy the physics goals must be obtained while using a 12-bit ADC. A multiple-gain system composed of one preamplifier followed by 4 amplifiers with gains 1, 5, 9 and 33 performs the analogue sampling: every 25 ns, the highest non-saturated gain is chosen and the analogue output is sent to a 12-bit flash ADC (Analog Devices), for digitization at 40 MHz. The fast shaping time of the pre-amplifier ($\sim$40 ns) is quite compatible with the 25 ns LHC rate constaint. The output of the ADC is serialized, then sent to the control room via an optical fiber (800 Mbits/s), where the trigger sum is performed. This design requires 1 fiber per crystal.

In 2002, the non-materialization of an anticipated drop in prices of optical data links necessitated a new design. The key element in the decision was the new radiation-hard 0.25 μm CMOS technology which allows the use of ASICs inside the detector at low cost. In the new design, shown in figure 5, the level-1 trigger primitive generation (energy sum of 25 crystals in the barrel) is moved from the control room onto the detector. The data are stored until a trigger is received, then only useful data are transferred. Only 3 optical links (data, trigger sum and control) per trigger tower (25 crystals in the barrel) are needed instead of 26 in the old design. The new design implies the development of a new FE card, with one new radiation-hard 0.25 μm ASIC (FENIX) for trigger sums and digital pipelining. The development has benefited from the experience gained by the CMS tracker group. The drawback is a more constrained design of the data acquisition and trigger systems. The second change concerns the FPPA. An important noise due to parasitic resistance and capacitance was affecting the first version of the FPPA. The problem was corrected in the last iteration and the noise is around 14000 e^-. But at that time, it was considered safer to develop an alternative to FPPA: the MGPA (MultiGain PreAmplifier) based on the 0.25 μm CMOS technology. One preamplifier is followed by 3 three amplifiers. The outputs are sent in parallel to a compound ASIC ADC (Chipidea) composed of 4 12-bits ADC. This considerably simplifies the design. In particular, only one power supply voltage is required. The new radiation-hard 0.25 μm tehchnology allow faster turnaround, higher yield and is less expensive. The drawback was the need to develop a new ADC. The first results are very promising, with a noise level probably around 8000 e^- for the barrel. This led the CMS collaboration to approve in July 2003 the MGPA solution as its new baseline for the ECAL electronics.

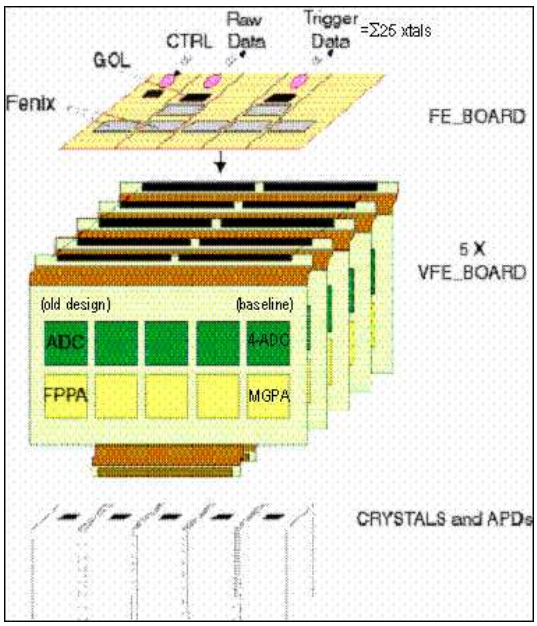

Figure 5: Schematic view of the readout electronics of a CMS ECAL tower

5 Laser Monitoring System

Crystal transparency is affected by radiation, but it is possible to monitor the loss and recovery of the light transmission by injecting a laser light into the crystal. This system will allow the correction of calibration constants between calibrations with physics events. The light of two laser systems at 440/495 nm and 700/800 nm with internal diagnostics on wavelength, pulse shape and intensity are distributed through a 2-level fanout system to each crystal via a radiation-hard optical link. The laser light is also sent to precision radiation hard PN diodes to take into account eventual laser fluctuations. Under irradiation the losses of the signal from the laser light (ΔL) and of the signal from beam particles (ΔB) are related by: $\frac{\Delta L}{L} = (\frac{\Delta B}{B})^{\alpha}$. The principle of the laser monitoring is based on the universality of α: α must be independent of time, and be homogeneous (*i.e.* the same for all crystals) to avoid becoming a new calibration constant. As a first approximation the energy resolution is related to the dispersion on α by $\frac{\delta E}{E} = \alpha \frac{\Delta L}{L} \frac{\delta \alpha}{\alpha}$. The complete monitoring system has been tested during the 2002 test-beam on a calorimeter module (M0') with 100 channels equipped with the FPPA FE electronics. A stability of 0.1% was achieved by the laser system. The α parameter was measured for 19 irradiated crystals as shown in figure 6. Despite the small statistics, it is a promising results concerning the universality of α. The observed dispersion of

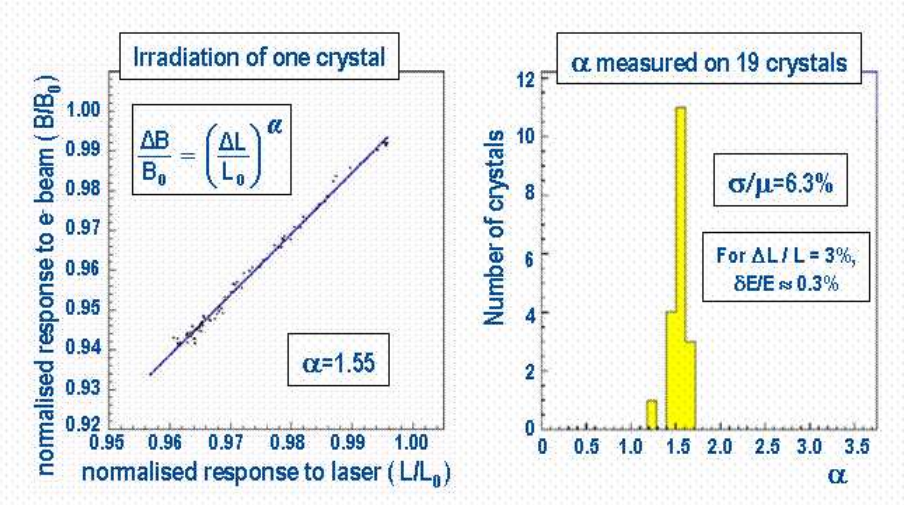

Figure 6: Left: Correlation between the relative drops of signal from 120 GeV electrons in one crystal and of the signal from laser light during an irradiation run. Right: Dispersion of the α parameter measured on 19 crystals.

6% on α is quite compatible with the limit fixed at 0.3% to the contribution of the laser monitoring system to the constant term of the energy resolution.

6 Other Testbeam Results

Temperature Stability - Another goal achieved during the 2002 testbeam is the temperature stability. The electromagnetic calorimeter will dissipate more than 200 kW. The strong temperature dependance of the crystal light yield (-2%/degree at $+18°$) and of the APD gain (-2.2%/degree) require a temperature stability better than $\pm 0.1°$. The temperature inside M0' was precisely studied with a large number of sensors placed in front of the crystal, at the interface between the crystals and the front-end electronics, and in the capsule close to the APDs. Figure 7 shows the temperature measured close to the APDs over a two-month period. The stability is well below the $0.1°$ limit. The small discontinuity observed is due to a powercut.

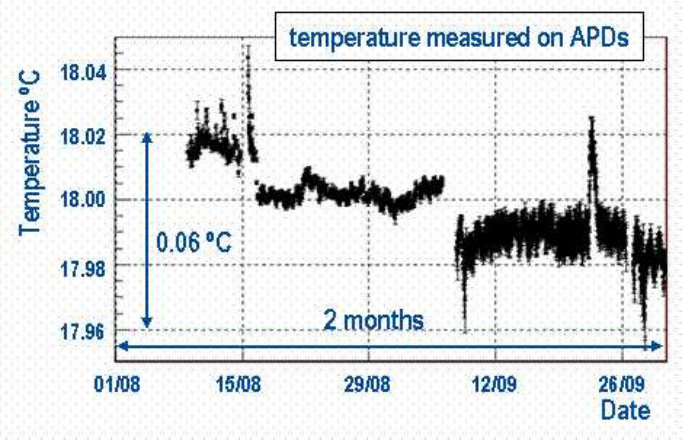

Figure 7: Temperature measured on APDs during a two-month period of testbeam.

Energy resolution - In 1999, a prototype of 30 crystals of the barrel calorimeter and a prototype of 25 crystals of the endcap were placed in beam [7]. They were equipped with non-final FE electronics. A non-radhard version of the preamplifier of the FPPA and a charge ADC were used. The endcap prototype was not preceded by a preshower. The following resolutions were obtained, consistent with design requirements as stated in the ECAL Technical Design Report [2]:

$$\frac{\sigma}{\mathrm{E}} = \frac{2.73\%}{\sqrt{\mathrm{E(GeV)}}} \oplus 0.42\% \oplus \frac{0.142}{\mathrm{E(GeV)}} \text{ (barrel)}$$

$$\frac{\sigma}{\mathrm{E}} = \frac{4.1\%}{\sqrt{\mathrm{E(GeV)}}} \oplus 0.25\% \oplus \frac{0.140}{\mathrm{E(GeV)}} \text{ (endcap)}$$

These results entirely validated the crystal-photodetector subset of the design.

7 Conclusion

After an intensive R&D program on crystals, photodetectors and very front-end electronics, the construction of the CMS ECAL, the largest crystal calorimeter ever built, is progressing well with more than 25% of the barrel crystals, more than 2/3 of the APDs and 1/3 of the VPTs already delivered. Beam tests have given very encouraging indications that the ambitious design goals can be met. The major redesign of the readout electronics architecture will be tested during summer 2003. Very recent preliminary results have established the functionality of the new architecture with on-detector trigger primitive generation. It is planned that the new VFE cards equipped with MGPAs will be tested during the October 2003 beam test, before the precalibration of a subset of the calorimeter supermodules in 2004.

References

[1] The LEP Electroweak Working Group, "A Combination of Preliminary Electroweak Measurements and Constaints on the Standard Model", LEPEWWG/2003-01

[2] The CMS Collaboration, "The Electromagnetic Calorimeter Project - Technical Design Report", CERN/LHCC 97-33

[3] E. Tournefier, "The Preshower Detector of CMS at LHC", presentation at Frontier detectors for Frontier Physics, 8th Pisa meeting on advanced detectors, Elba, Italy, May 21-27, 2000, CMS CR-2000/010.

[4] X. Qu *et al.*, "Radiation Induced Color Centers and Light Monitoring for Lead Tungstate Crystals", CMS NOTE 1999/069.

[5] R. Rusack, "Avalanche Photodiodes for the CMS Lead Tungstate Calorimeter", presentation at CALOR2002, Caltech, 25-30 May 2002.

[6] R.M. Brown *et al.*, "The development of vacuum phototriodes for the CMS electromagnetic calorimeter", Nucl. Instr. and Meth. **A469** (2001) 29-46.

[7] P. Depasse *et al.* "Analysis from August 1999 Beam Tests of a $PbWO_4$ Crystal Matrix", CMS NOTE 2000-009